

# Low Frequency Spinning LiDAR De-Skewing

Omar Salem   Emanuele Giacomini   Leonardo Brizi   Luca Di Giammarino   Giorgio Grisetti

**Abstract**—Most commercially available Light Detection and Ranging (LiDAR)s measure the distances along a 2D section of the environment by sequentially sampling the free range along directions centered at the sensor’s origin. When the sensor moves during the acquisition, the measured ranges are affected by a phenomenon known as “skewing”, which appears as a distortion in the acquired scan. Skewing potentially affects all systems that rely on LiDAR data, however it could be compensated if the position of the sensor were known each time a single range is measured. Most methods to de-skew a LiDAR are based on external sensors such as IMU or wheel odometry, to estimate these intermediate LiDAR positions. In this paper we present a method that relies exclusively on range measurements to effectively estimate the robot velocities which are then used for de-skewing. Our approach is suitable for low frequency LiDAR where the skewing is more evident. It can be seamlessly integrated into existing pipelines, enhancing their performance at negligible computational cost. We validated the proposed method with statistical experiments characterizing different operating conditions and we release an open source C++ implementation.

## I. INTRODUCTION

Accurate and reliable mapping, localization, and navigation are essential for a wide range of robotics applications from autonomous driving, logistics, search and rescue, and many others. To this extent, LiDAR sensors are a popular choice since they allow to sense both the free space and the location of obstacles around the robot.

Two are the main operating principles for LiDARs: Time of Flight (ToF) and triangulation. ToF devices operate by measuring the round trip time and phase of a laser pulse sent along a direction. Triangulation LiDARs measures the disparity of the endpoint of the laser beam through a linear camera mounted aside the emitter [2]. The range of an object is then proportional to the reciprocal of the disparity, hence their accuracy decreases with the range.

Regardless the principle used to measure the distance along one direction, to sense a perimeter the LiDAR measurement should be deflected. In case of ToF LiDARs this is done by deflecting the laser beam on a plane by a rotating mirror, while triangulation devices rotate the entire sensor head. In the remainder of this work we will refer to these devices as *spinning* LiDARs. The prices of LiDARs vary greatly, depending on the technology used, on the range and on the fact that they are 2D or 3D.

In this work we focus on low grade hobby LiDARs such as the InnoMaker-LD-06 or the RPI-Lidar A1 that can be bought for less than 100 Eur at the time of writing. The major shortcoming of these devices is their relatively slow

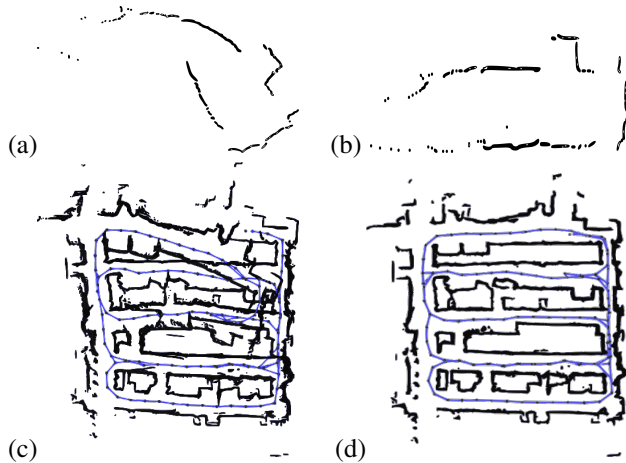


Fig. 1: Effects of a the de-skewing. Top: (a) unprocessed scan acquired by a moving robot, (b) same scan de-skewed by using our approach. Bottom: (c) map build by a SLAM algorithm on skewed scans, (d) map obtained by the same SLAM algorithm using scans de-skewed with our method.

rotational speed that results in a full sweep of measurements becoming available between 5 to 13 Hz. In contrast to more expensive models these devices are not equipped with an inertial unit or other means to estimate the proprioceptive motion of the sensor while it moves.

In spinning LiDARs, the scan acquisition is not instantaneous, hence the origin of the beam in the world frame changes for each sensed range. Assuming that all measurements gathered during one rotation are sampled at the same time results in a distorted or skewed scan. Since most perception blocks in a navigation system, such as SLAM or localization treat the scans as rigid bodies, the effect of skewing leads to undesirable decay in accuracy that can be so severe to result in failures as analyzed by Al-Nuaimi *et al.* [1].

A common way to compensate for the motion of the LiDAR while it rotates is to integrate external proprioceptive measurements (dead reckoning and/or Inertial Measurement Unit (IMU)), to estimate the origin and orientation of the laser beam each time a range is acquired [6], [17], [10]. High-end 3D LiDARs already contain a synchronized IMU, which is not available on the inexpensive models previously mentioned.

In this paper, we propose an approach to estimate the velocities at which the robot where the LiDAR is mounted moves, based *solely* on the range measurements, that are processed as a stream. Our method is based on a non-rigid plane-to-plane registration algorithm, where the velocity of

the platform carrying the sensor is estimated by maximizing the geometric consistency of the stream of ranges. We conducted several statistical experiments on real and synthetic data. Results show that our de-skewing method is effective estimating the motion of the robot, enhancing the quality of Simultaneous Localization and Mapping (SLAM) and localization estimates, at negligible computation.

We release an open source C++ implementation of our method as a plug-and-play component that can be added to existing 2D LiDAR pipelines. In Fig. 1 we illustrate the effects of our approach both on individual measurements, and when used within a more complex SLAM system. In the remainder of this paper we first review the related work in Sec. II, subsequently we describe in detail our de-skewing method for 2D LiDAR data (Sec. III). We conclude the paper with a broad set of experiments aimed at measure the performances of our method under different operating conditions (Sec. IV), and finally, we draw some conclusions on the benefits and the limitations of our approach.

## II. RELATED WORK

In this section, we review the most recent approaches to de-skew LiDAR data. Existing approaches for de-skewing mostly use either wheeled odometry or IMU to estimate the relative motion of the sensor/robot while a scan is being acquired. This process involves motion integration, that might result in an unbounded growth of the estimate’s error. In addition, consumer-grade IMU are Micro-electromechanical Systems (MEMS), and suffer from thermal variations and other disturbances, resulting in continuously changing measurement biases. Thanks to the dominant effect of gravity, the IMU have a constant reference for the attitude, allowing the integration of the angular velocity along the yaw direction obtained by integrating the gyroscope, to be relatively stable in the short term. In contrast, the position estimate is not usable, unless performing periodic bias correction.

The majority of works addressing de-skewing with wheeled odometry or IMU rely on some estimators that processes the raw proprioceptive data such as a filter or an integrator that directly provides an estimate of the sensor position each time a single range is measured. These methods fall in the class of *loosely-coupled*, since they do not use the LiDAR information to refine the proprioceptive estimate. Among this class we find the work of Tang *et al.* [12] that proposes to match subsequent scans to compute a relative motion, where the initial relative orientations are provided by an IMU. The two scans are registered twice: the first time to determine the velocity of the robot between the two time instants, and the second time the scans de-skewed with the estimated velocities are registered to determine the final motion. Subsequently, He *et al.* [6] proposed a method to estimate relative motion between IMU poses and de-skew subsequent ranges by using these smoothed poses. Some of the key advantages of these approaches is that are computationally cheap and straightforward to implement. On the other hand, they are very sensible and often fail in more complex scenario.

In contrast to loosely-coupled approaches, *tightly-coupled* methods jointly process LiDAR and IMU. These methods are typically based on either smoothing or filtering. Wei *et al.* [15] uses a pre-integration scheme to estimate the LiDAR’s ego-motion based on the inertial measurements, and updates the IMU biases in the correct step of an iterative EKF whenever a scan is completed. Shan *et al.* [11] includes the states of IMU in the factor-graph, updating IMU biases through the optimization process, adapting a well known computer vision work [5] to the LiDAR case. This ideas have been further extended in [13], [16] where the authors resort to full factor-graph optimization to obtain a state configuration that is maximally consistent with all the IMU measurements and LiDAR ranges. Tightly-coupled approaches are typically more robust w.r.t. their loosely-coupled counterpart. However this comes at a relevant relative cost, both in terms of computation and ease of implementation.

Generally, to take advantage from additional sensors, such as IMU or wheeled odometry for LiDAR in the de-skewing process, one requires an accurate time synchronization between the sensors. Unfortunately, this is not straightforward to obtain on inexpensive small devices such as RPI LiDAR or LD-06 due to effect such as latencies on the communication subject that might vary depending on the computational load of the computer. These issues, however, can be completely avoided when using only LiDAR data to perform de-skewing. At their core LiDAR only methods have a registration algorithm, whose aim is to compute the velocities of the sensor while the robot moves. The basic intuition is that if the correct velocities were found, the sequence of range measurements could be assembled in a maximally consistent scan. In this context one Moosman *et al.* [9] propose to estimate the motion between a pair skewed scans, subsequently they interpolate linearly the sensor’s pose between the two estimates to de-skew each range measurement and finally re-align the de-skewed pairs. Albeit effective this method recovers the velocities by linear interpolation based on a potentially non optimal alignment obtained from two skewed scans. This double approximation might hinder the accuracy when the initial registration fail, resulting in even worse estimates. Al-Nuaimi *et al.* [1] provide a mathematical analysis of scan skewing and an approach to lessen the effect of skewing during registration. To this extent, they propose a weighting schema based on their adapted Geometric Algebra LMS solver, associating clouds using a point-to-plane approach. However, they assume that consecutive translation and rotational motion are equal over time. Both these two approaches are designed for high-frequency 3D LiDARs. From the best of our knowledge, there are no works in literature addressing the de-skewing problem on slow and inexpensive devices. Recently, Wu *et al.* [14] presented a work relatively close to our approach operating on a more complex 3D scenario, and leveraging on a similar registration method. However, this work relies on Frequency Modulated Continuous Wave (FMCW) devices that return Doppler velocity measurements for the LiDAR endpoints. Such a technology is currently not available on

low end devices.

In this paper, we propose a planar LiDAR-only approach that addresses the de-skewing problem by continuously registering the sequence of range measurements. The registration is carried on by estimating the LiDAR’s planar velocity, which iteratively minimizes a plane-to-plane metric between the de-skewed endpoints. Our results demonstrate that our methodology is accurate in estimating the velocity of the robot, only based on the laser measurements. Furthermore, we show that using our method effectively enhances existing 2D LiDAR-based SLAM and localization systems.

### III. OUR APPROACH

As stated in the introduction, to effectively de-skew a set of range measurements, one requires a reasonable estimate of the sensor position when each of the measurements was taken. Our method leverages some mild assumptions about the motion of the sensor mounted on the robot and the structure of the environment to operate on a continuous stream of range measurements. More specifically we assume to have a spinning planar LiDAR sensor. Hence, we define each measurement as  $\mathbf{z}_i = \langle r_i, \alpha_i, t_i \rangle$ . Here,  $r_i$  is the range,  $\alpha_i$  is the angle of the laser beam with respect to the origin of the sensor and  $t_i$  is the timestamp. We assume the environment consists of a locally smooth surface and that the robot velocities change mildly within a LiDAR beam revolution.

If we knew the rotational and translational velocities of the robot during the motion, we could integrate them to estimate a local chunk of trajectory, addressing the laser de-skewing problem. Our method estimates these velocities by registering the stream of measurements  $\{\mathbf{z}_i\}$  onto itself. The most likely velocities are the ones that, if applied for de-skewing renders the measurement maximally consistent. Consistency is measured by a plane-to-plane metric applied between the corresponding portions of the scans. More formally, let  $\mathbf{x} = (v \ \omega)^T$  be the linear and angular velocity of the robot we want to estimate, such that

$$\mathbf{x}^* = \underset{\mathbf{x}}{\operatorname{argmin}} \sum_{(i,j) \in \mathcal{C}} \rho \|\mathbf{e}(\mathbf{x}, t_i, t_j)\|^2. \quad (1)$$

Where  $\mathbf{e}(\mathbf{x}, t_i, t_j)$  denotes an error vector between two planar scan patches computed around two corresponding measurements at time  $t_i$  and  $t_j$ . The optimization step estimates new velocities  $\mathbf{x} = (v \ \omega)^T$  under the current set of correspondences  $\mathcal{C}$ , using Gauss-Newton (GN) as iteration strategy in our Iterative Least-Squares (ILS) problem. In Eq. (1)  $\rho$  denotes the Huber robust estimator.

Our algorithm is an instance of Iterative Closest Point (ICP) since it proceeds by alternating between the optimization and data association steps. Predicting an initial guess of correspondences, we estimate velocities using the constructed midpoints normal vectors. Measurements are then de-skewed, and used to search for better correspondences that will minimize our error metric iteratively.

In the remainder of this section, we will detail the different steps. In Sec. III-A we will review how to compute the posi-

tion of the sensor, given the velocities, and we briefly recall how to de-skew a stream of measurements. Subsequently, in Sec. III-B we detail our error metric and we outline the necessary regularization that has to be carried out on the raw input. Finally, in Sec. III-C we illustrate our heuristic to compute the associations.

#### A. Velocity Based De-skewing

Whereas our approach can be applied to more complex kinematics, for the sake of simplicity we detail the common case of a unicycle mobile base. Our goal is to estimate the location  $\mathbf{T}(\mathbf{x}, t_i) = (x_i \ y_i \ \theta_i)^T$  of the mobile base at time  $t_i$ , assuming it starts from the origin and progresses with constant linear and rotational velocities over sampling time  $\mathbf{x} = (v \ \omega)^T$ . After a time  $t_i$ , the robot would have traveled for a distance  $l_i = v \cdot t_i$  and its angle is  $\theta_i = \omega \cdot t_i$ . The base will move along an arc whose radius is  $R$ . We can calculate the radius of the arc  $R$  as

$$R = \frac{v_i}{\omega_i} = \frac{l_i}{\theta_i}. \quad (2)$$

From this consideration, we can easily compute  $\mathbf{T}$  as

$$\mathbf{T}(\mathbf{x}, t_i) = \begin{pmatrix} R \sin \theta_i \\ R(1 - \cos \theta_i) \end{pmatrix} = \underbrace{v \cdot t_i}_{l_i} \begin{pmatrix} \frac{\sin \theta_i}{\theta_i} \\ \frac{1 - \cos \theta_i}{\theta_i} \end{pmatrix} \quad (3)$$

Assuming the sensor (LiDAR) is located at the center of the mobile base, if at time  $t_i$  the beam has a relative angle  $\alpha_i$  and reports a range measurement  $r_i$ , we can straightforwardly find the 2D laser endpoint  $\mathbf{p}_i$  as follows:

$$\mathbf{p}_i(\mathbf{x}, t_i) = \mathbf{R}(\theta_i + \alpha_i) \begin{pmatrix} r_i \\ 0 \end{pmatrix} + \begin{pmatrix} x_i \\ y_i \end{pmatrix}. \quad (4)$$

Here  $\mathbf{R}(\theta_i + \alpha_i) \in SO(2)$  is 2D rotation matrix of  $\theta_i + \alpha_i$ . Applying this process to all the measurements and mapping all reconstructed points back to the pose where the acquisition of the current scan was started, results in the desired de-skew operation.

#### B. Error Metric

To evaluate a plane-to-plane distance the algorithm needs to compute the normal vectors, which are based on the endpoints. Since the position of the endpoints is a function of the estimated velocities  $\mathbf{x}$ , also the normal vectors are. Hence the algorithm has to recompute both endpoints and normals at each iteration. Furthermore, when subsequent endpoints are too close, the noise affecting the range might result in an unstable normal vector, which hinders the error metric. To lessen this effect, before each iteration we regularize the scan to retain only temporally subsequent measurements that are sufficiently far from each other to ensure a stable normal. In our experiments, we set this threshold to 0.15 m. Similarly, if there is a large distance gap between two subsequent endpoints ( $>0.4$  m), likely, the surface is not continuous at that point, hence we drop those measurements too.

At the end of this regularization step, we end up with a set of reasonably stable measurements we can use for the remainder of the computation. For each temporally

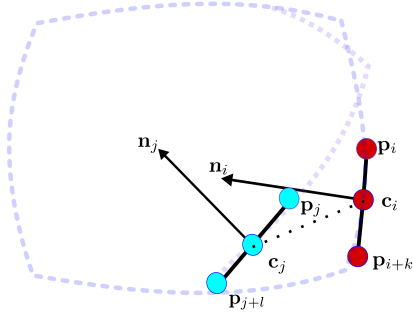


Fig. 2: Illustration of the planar patches calculation and of the correspondence search between two matching patches at  $\mathbf{m}_i$  and  $\mathbf{m}_j$ .

subsequent pair of endpoints, we compute a planar patch  $\mathbf{m}_i = \langle \mathbf{c}_i, \mathbf{n}_i, t_i \rangle$ , characterized by a center  $\mathbf{c}_i$ , a normal vector  $\mathbf{n}_i$ , and a timestamp  $t_i$ , such that:

$$\mathbf{c}_i = \frac{1}{2} (\mathbf{p}_{i+k} + \mathbf{p}_i), \quad (5)$$

$$\mathbf{n}_i = \begin{pmatrix} 0 & 1 \\ -1 & 0 \end{pmatrix} \frac{\mathbf{p}_{i+k} - \mathbf{p}_i}{\|\mathbf{p}_{i+k} - \mathbf{p}_i\|}, \quad (6)$$

$$t_i = \frac{1}{2} (t_{i+k} + t_i). \quad (7)$$

Here, the index  $k > 0$  accounts for endpoints suppressed during regularization. If two planar patches  $\mathbf{m}_i$  and  $\mathbf{m}_j$  are related to the same portion of the environment, we can calculate an error vector  $\mathbf{e}(\mathbf{x}, t_i, t_j)$  accounting for their both their distance and difference in orientation. The error vector is a function of the velocities, since the patches  $\mathbf{m}_i$  and  $\mathbf{m}_j$  are computed based on the endpoints. The latter are related to the velocities by Eq. (4).

Let  $\mathbf{e}(\mathbf{x}, t_i, t_j) \in \mathbb{R}^3$  be such an error vector, whose components are defined as follows:

$$\mathbf{e}(\mathbf{x}, t_i, t_j) = \begin{pmatrix} \frac{1}{2}(\mathbf{c}_i - \mathbf{c}_j)^T(\mathbf{n}_i + \mathbf{n}_j) \\ \mathbf{n}_j - \mathbf{n}_i \end{pmatrix}. \quad (8)$$

Here the first dimension accounts for the distance between two corresponding planar patches  $\mathbf{m}_i$  and  $\mathbf{m}_j$  projected along the average of their normals. The other two accounts for the difference between the normal vectors. Eq. (8) is differentiable in the velocities  $\mathbf{x}$ , hence we can minimize Eq. (1) by Iterative Reweighted Least Squares.

### C. Data Association

To determine the correspondence we proceed at each iteration by de-skewing the sequence of measurements, to get a set of updated endpoints  $\mathbf{p}_i$ . Subsequently, we apply the regularization to discard those measurements whose endpoints fall either too close or too far from their temporal neighbors. This gives us a set of sequential stable measurements we can use to compute the patches  $\mathbf{m}_i$ .

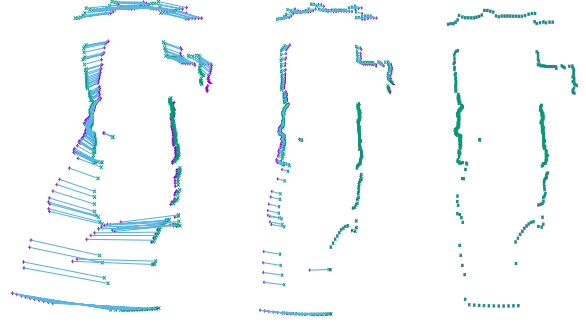


Fig. 3: Iterative evolution of the de-skewing process. Left: initial configuration, Middle: after 4 iterations, Right: after 25 iterations.

Once this is done, for each  $\mathbf{m}_i$  we seek for those other patches  $\mathbf{m}_j$  that fulfill all the following criteria:

- their centers are close enough  $|\mathbf{c}_i - \mathbf{c}_j| < \tau_c$ ,
- their normals are sufficiently parallel  $\mathbf{n}_i \cdot \mathbf{n}_j > \tau_n$ ,
- their timestamp are sufficiently distant  $|t_i - t_j| > \tau_t$ .

Within this set we select as correspondence for  $\mathbf{m}_i$  the  $\mathbf{m}_j$  having the smallest projective distance  $(\mathbf{c}_i - \mathbf{c}_j)^T(\mathbf{n}_i + \mathbf{n}_j)$ . Fig. 3 shows subsequent iterations of the our approach.

## IV. EXPERIMENTAL EVALUATION

In this section, we present a set of quantitative and qualitative evaluations to measure:

- the accuracy of the velocities estimated by our approach, which is directly responsible for the reliability of the de-skewed scan. To this extent we carried out a set of statistical experiments under changing velocities;
- the accuracy of SLAM and localization tasks when coupled with our de-skewing method.

To quantitatively carry on the evaluations we used our own implementation of a simulator capturing the behavior of a slowly rotating 2D LiDAR mounted on a mobile platform. The maps are generated from real-world data, using high-end LiDARs.

We recall that the main parameter influencing the skew effect is the ratio between the rate of the sensor and the velocity of the robot carrying the sensor. Hence, during all experiments using synthetic data, we varied both the rotational velocity and translational velocities of the robot while keeping the LiDAR at a frequency of 5 full scans per second.

To validate the results obtained in simulation, we carried on real-world experiments by using a self-built differential drive mobile robot, equipped with a LD-06 LiDAR running at 10 Hz. We compare the velocities estimated by our approach with those provided by our accurate wheeled odometry, which is the result of an automatic calibration process [3]. In all experiments, our method was operating on a window of measurements including two full rotations of the mirror (two full scans).

$\omega_{gt}$	$\omega_{est}$ (mean/std)	$S_{RMSE}$	$D_{RMSE}$
-2.000	-1.981/0.023	1.543	0.094
-1.000	-0.992/0.015	0.827	0.054
-0.500	-0.495/0.009	0.568	0.043
0.500	0.496/0.013	0.460	0.054
1.000	0.993/0.015	0.789	0.061
2.000	1.990/0.022	1.409	0.091

TABLE I: Evaluation of the angular velocity estimate under a pure rotational motion.  $\omega_{gt}$  and  $\omega_{est}$  are ground truth and estimated angular velocities, while  $S_{RMSE}$  and  $D_{RMSE}$  are the point to point RMSE for skewed scan and for de-skewed scans respectively.

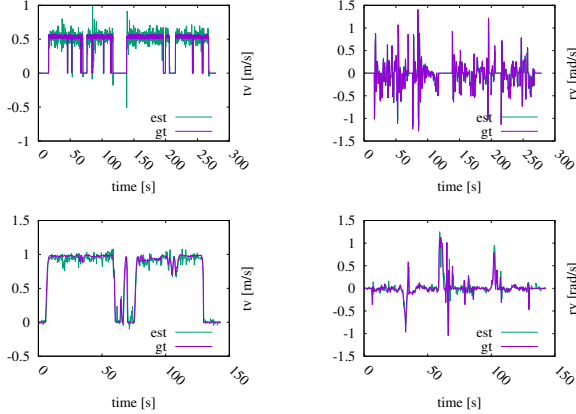


Fig. 4: Evolution of estimated and real velocities. Top Row: synthetic data, bottom row: real data. Left column: translational velocity, Right column: rotational velocity.

#### A. Velocity estimation

The goal of this experiment is to compare the velocities of the robot calculated by our approach with the ground truth available from the simulator. To this extent, we impose the robot to move with constant pure velocities (i.e. only rotational velocity or only translational velocity) in different portions of the map. In addition, we measured how close a de-skewed scan is with respect to its ground truth counterpart. To this extent, we run the same de-skewing procedure twice per scan. The first time we compute the ground truth measurement by setting the applied velocities (available from the simulator), and the second time we compute the de-skewed scan by using our velocity estimate. The consistency is measured as the distance between corresponding endpoints in the two scans. Tab. I and Tab. II report respectively rotational and translational results. Fig. 4 shows the temporal evolution of the estimated velocities during a typical simulated run.

We repeated this experiment on the real robot and the velocity plots in Fig. 4 confirm that our system can effectively recover the robot’s velocities, correctly de-skewing the scan.

Generally, we observed that our de-skewing approach behaves differently depending on the sign of the rotational velocity applied to the robot. If the robot and the LiDAR rotate in the same direction, the effective beam angular rate is increased. For this reason, during the time of two full rotations, the beam captures more than twice the same portion of the environment shown in Fig. 1, resulting in lower

$v_{gt}$	$v_{est}$ (mean/std)	$S_{RMSE}$	$D_{RMSE}$
5.000	4.442/1.403	0.568	0.433
3.000	2.778/0.661	0.502	0.185
2.000	1.890/0.428	0.459	0.252
1.500	1.440/0.264	0.442	0.227
1.000	0.974/0.147	0.435	0.171
0.500	0.494/0.078	0.366	0.201

TABLE II: Evaluation of the translational velocity estimate under purely linear motion.  $v_{gt}$  and  $v_{est}$  are ground truth and estimated translational velocities, while  $S_{RMSE}$  and  $D_{RMSE}$  are the point to point RMSE for skewed scan and for de-skewed scans.

$v_{max}/\omega_{max}$	$t_{gt}$	$t_S$	$t_D$
0.5/0.5	11.427	14.845	13.832
0.5/1.0	7.417	8.020	7.426
1.0/1.0	5.643	9.887	7.373
1.0/2.0	6.067	6.481	6.903
2.0/2.0	5.816	6.032	5.829

TABLE III: Global localization convergence time for different maximum velocities ( $v_{max}, \omega_{max}$ ).  $t_{gt}$ ,  $t_S$ , and  $t_D$  indicate respectively the convergence time with the ground truth scan, with the skewed raw scan and by using our approach.

error. In contrast, when the velocities are opposite, it might be that during two rotations the support is too small for the data association heuristic to succeed, hence leading to worse results. Results show that applying our approach on slow planar LiDAR, lead to good velocities estimate that allow the LiDAR scan to be more consistent compared with the ground truth.

#### B. Localization

The experiment aims at measuring the benefits of our de-skewing approach in the context of global localization. To this extent, we processed the synthetic data acquired during the SLAM run, and we measured the time required by the global localization covariance determinant to converge under a certain threshold ( $\leq 0.0001$ ). As localizer we used our implementation of a particle filter [8], initially bootstrapped with 3000 particles.

Our conjecture is that having input data more similar to the map, results in sharper likelihood functions and faster convergence. Tab. III confirms this.

$v_{max}/\omega_{max}$	$v_{est}/\omega_{est}$	$S/D$	$ATE^S/ATE^D$
0.5/0.5	0.102/0.138	0.418/0.246	0.329/0.113
0.5/1.0	0.140/0.334	0.529/0.265	0.246/0.232
1.0/1.0	0.282/0.389	0.543/0.308	1.018/0.977
1.0/1.5	0.322/0.502	0.566/0.321	1.586/1.520
2.0/2.0	0.516/0.760	0.618/0.414	11.18/1.805

TABLE IV: Results of the SLAM experiments, conducted with different maximum velocities ( $v_{max}/\omega_{max}$ ). The table reports the RMSE for the estimated translational and rotational velocities ( $v_{est}/\omega_{est}$ ), the endpoint errors of the skewed ( $S$ ) and de-skewed scans ( $D$ ), and finally the RMSE of the Absolute Trajectory Error measured by feeding SLAM with skewed ( $ATE^S$ ) and de-skewed ( $ATE^D$ ) data.



Fig. 5: SLAM Results. Left: map with ground truth scans, Middle: map with raw scans, Right: map with scans de-skewed by our approach.

### C. SLAM

In our final experiment, we used our de-skewing mechanism to pre-process the input of our 2D LiDAR SLAM system [4]. We run SLAM on three different inputs: the raw (skewed) scans, the ones de-skewed by using our approach, and on the data de-skewed by using the ground truth. We simulated different exploration runs of the same environment while changing the velocity bounds of the robot. Fig. 5 illustrates the three different maps obtained, while Tab. IV quantitatively summarizes the results of this experiment where we report the RMSE of the velocity estimates, the RMSE of the endpoint error for both the skewed and de-skewed data.

Furthermore we measure the Absolute Trajectory Error (ATE) between the ground truth trajectory computed with by the simulator and the ones estimated by SLAM by using the two types of scans. ATE measures the distance between corresponding points of the trajectories, after computing a transformation that makes them as close as possible. For trajectory registration we used Horn method [7], while the corresponding poses are associated with the timestamps. The results are summarized in Tab. IV. The RMSE of the velocity estimates is reasonably small, while the endpoint error is substantially reduced by our de-skewing method. Consistently, the trajectories obtained by using de-skewed data are substantially close to the ground truth than their skewed counterpart. This is confirmed by the maps generated based on the trajectories and illustrated in Fig. 5. These results are consistent with the intuition that using skewed scans when doing SLAM is not recommended, since these measurements might induce systematic unrecoverable errors in the registration process.

## V. CONCLUSION

In this paper, we presented a simple and effective planar LiDAR de-skewing mechanism based on some plane-to-plane registration criteria. To the best of our knowledge, this is the only de-skewing pipeline that does not rely on additional sensors (i.e. IMU, wheel encoders), targeting specifically slow and inexpensive LiDAR enhances the quality of the scan, always improving the performances of existing SLAM and localization algorithms. We release our software as a C++ open-source package.

## REFERENCES

[1] A. Al-Nuaimi, W. Lopes, P. Zeller, A. Garcea, C. Lopes, and E. Steinbach. Analyzing lidar scan skewing and its impact on scan matching.

In *2016 International Conference on Indoor Positioning and Indoor Navigation (IPIN)*, pages 1–8. IEEE, 2016.

[2] C. Cajal, J. Santolaria, D. Samper, and A. Garrido. Simulation of laser triangulation sensors scanning for design and evaluation purposes. *International Journal of Simulation Modelling (IJSIMM)*, 14(2):250–264, 2015.

[3] M. Di Cicco, B. Della Corte, and G. Grisetti. Unsupervised calibration of wheeled mobile platforms. In *Proc. of the IEEE/RSJ Int. Conf. on Intelligent Robots and Systems (IROS)*, 2016.

[4] M. Colosi, I. Aloise, T. Guadagnino, D. Schlegel, B. Della Corte, K.O. Arras, and G. Grisetti. Plug-and-play slam: A unified slam architecture for modularity and ease of use. In *Proc. of the IEEE/RSJ Int. Conf. on Intelligent Robots and Systems (IROS)*, pages 5051–5057, 2020.

[5] C. Forster, L. Carlone, F. Dellaert, and D. Scaramuzza. On-manifold preintegration for real-time visual-inertial odometry. *IEEE Transactions on Robotics (T-RO)*, 33(1):1–21, 2016.

[6] L. He, Z. Jin, and Z. Gao. De-skewing lidar scan for refinement of local mapping. *Sensors*, 20(7):1846, 2020.

[7] B. Horn, H. Hilden, and S. Negahdaripour. Closed-form solution of absolute orientation using orthonormal matrices. *Journal of the Optical Society of America A (JOSA A)*, 5(7):1127–1135, 1988.

[8] M. T. Lázaro, G. Grisetti, L. Iocchi, J. P. Fentanes, and M. Hanheide. A lightweight navigation system for mobile robots. In Anibal Ollero, Alberto Sanfeliu, Luis Montano, Nuno Lau, and Carlos Carreira, editors, *ROBOT 2017: Third Iberian Robotics Conference*. Springer International Publishing, 2018.

[9] F. Moosmann and C. Stiller. Velodyne slam. In *Intelligent Vehicles Symposium (IV)*, pages 393–398. IEEE, 2011.

[10] T. Shan and B. Englot. Lego-loam: Lightweight and ground-optimized lidar odometry and mapping on variable terrain. In *Proc. of the IEEE/RSJ Int. Conf. on Intelligent Robots and Systems (IROS)*, pages 4758–4765. IEEE, 2018.

[11] T. Shan, B. Englot, D. Meyers, W. Wang, C. Ratti, and D. Rus. Lio-sam: Tightly-coupled lidar inertial odometry via smoothing and mapping. In *Proc. of the IEEE/RSJ Int. Conf. on Intelligent Robots and Systems (IROS)*, pages 5135–5142. IEEE, 2020.

[12] J. Tang, Y. Chen, X. Niu, L. Wang, L. Chen, J. Liu, C. Shi, and J. Hyypä. Lidar scan matching aided inertial navigation system in gnss-denied environments. *Sensors*, 15(7):16710–16728, 2015.

[13] Z. Wang, L. Zhang, Y. Shen, and Y. Zhou. D-liom: Tightly-coupled direct lidar-inertial odometry and mapping. *IEEE Transactions on Multimedia (TMM)*, 2022.

[14] Y. Wu, D.J. Yoon, K. Burnett, S. Kammel, Y. Chen, H. Vhavle, and T.D. Barfoot. Picking up speed: Continuous-time lidar-only odometry using doppler velocity measurements. *IEEE Robotics and Automation Letters (RA-L)*, 8(1):264–271, 2022.

[15] W. Xu and F. Zhang. Fast-lio: A fast, robust lidar-inertial odometry package by tightly-coupled iterated kalman filter. *IEEE Robotics and Automation Letters (RA-L)*, 6(2):3317–3324, 2021.

[16] H. Ye, Y. Chen, and M. Liu. Tightly coupled 3d lidar inertial odometry and mapping. In *Proc. of the IEEE Int. Conf. on Robotics & Automation (ICRA)*, pages 3144–3150. IEEE, 2019.

[17] J. Zhang and S. Singh. Loam: Lidar odometry and mapping in real-time. In *Robotics: Science and Systems (RSS)*, volume 2, pages 1–9. Berkeley, CA, 2014.